MicroPET Imaging of Gene Transfer with a Somatostatin Receptor–Based Reporter Gene and ^{94m}Tc-Demotate 1

Buck E. Rogers, PhD[1]; Jesse J. Parry, BS[1]; Rebecca Andrews[1]; Paul Cordopatis, PhD[2]; Berthold A. Nock, PhD[3]; and Theodosia Maina, PhD[3]

[1]*Department of Radiation Oncology, Washington University School of Medicine, St. Louis, Missouri;* [2]*Department of Chemistry, University of Patras, Patras, Greece; and* [3]*Institute of Radioisotopes–Radiodiagnostic Products, National Center for Scientific Research Demokritos, Athens, Greece*

Gene therapy trials would benefit greatly from the use of noninvasive imaging to determine the location, magnitude, and time course of gene transfer. Somatostatin receptor subtype 2 (SSTR2) has been used as a reporter probe for γ-camera imaging of gene transfer in animal models. PET has greater sensitivity than γ-camera imaging and therefore would have an advantage for the imaging of SSTR2 gene transfer. **Methods:** An adenovirus (AdHASSTR2) carrying *sstr2*, which encodes an N-terminal hemagglutinin epitope, was used for evaluating SSTR2 gene transfer. The somatostatin analog Demotate 1 (Tyr^3-octreotate conjugated to the 1,4,8,11-tetraazaundecane chelator) was used for chelation of the positron emitter ^{94m}Tc (half-life, 52 min) and targeting to SSTR2. Gene transfer was evaluated in vitro with A-427 non–small cell lung cancer cells after infection with AdHASSTR2 by ^{94m}Tc-Demotate 1 binding and internalization assays. In vivo biodistribution and microPET studies were conducted with mice bearing A-427 tumor xenografts directly injected with AdHASSTR2 to determine the tumor localization of ^{94m}Tc-Demotate 1. **Results:** ^{94m}Tc-Demotate 1 bound with high affinity and was internalized rapidly into AdHASSTR2-infected A-427 cells. Biodistribution studies showed uptake of ^{94m}Tc-Demotate 1 in tumors infected with AdHASSTR2 (4.0 percentage injected dose per gram [%ID/g] at 2 h) and background uptake in tumors infected with a control adenovirus (0.8 %ID/g at 2 h). The uptake of ^{94m}Tc-Demotate 1 in AdHASSTR2-infected tumors was greater than the uptake in all other tissues, except for the kidneys and the SSTR2-positive pancreas. MicroPET imaging showed similar results, with clear uptake of ^{94m}Tc-Demotate 1 in AdHASSTR2-infected tumors, background uptake in control tumors, and clearance through the kidneys. **Conclusion:** These studies show that the positron-emitting somatostatin analog ^{94m}Tc-Demotate 1 could be used to determine SSTR2 gene transfer by microPET imaging, a result that will improve the sensitivity of the SSTR2 reporter gene system.

Key Words: somatostatin receptor; gene transfer; PET; ^{94m}Tc; adenovirus

J Nucl Med 2005; 46:1889–1897

In more than 600 clinical gene therapy trials worldwide in the past 15 y, approximately 3,500 patients have been treated (according to the *Journal of Gene Medicine* Web site, at www.wiley.co.uk/genetherapy/clinical). More than 500 of the trials have been conducted in the United States, and 400 have been carried out in the context of the treatment of cancer. Retroviral vectors were used as gene delivery vehicles in 34% of the protocols, whereas adenoviral vectors were used in 27%. It is clear that gene therapy will be evaluated clinically as an approach for the treatment of numerous human disorders despite obstacles that must be overcome before gene therapy can live up to its potential (*1*). One obstacle that must be overcome is the ability to determine whether gene transfer has occurred in an individual patient (*2*). Biopsies are taken to determine whether gene transfer has occurred, but this process is invasive and does not yield spatial or temporal patterns of gene expression. Therefore, noninvasive imaging of gene transfer would determine whether gene transfer has occurred in a patient, what tissues have been transduced, and the magnitude and time course of gene expression (*2*).

Several groups are developing methods for noninvasively imaging gene transfer. In general, these methods have focused on nuclear imaging, MRI, and optical imaging (*3*). Each imaging technology has various advantages and limitations. We have focused on nuclear imaging with the human somatostatin receptor subtype 2 (SSTR2) gene as a reporter gene, although many nuclear imaging studies of gene transfer have been carried out with the herpes simplex virus type 1 thymidine kinase (*4,5*), the dopamine 2 receptor (*6,7*), and the sodium iodide symporter (*8,9*) genes as reporter genes. Five somatostatin receptor subtypes (SSTR1–

Received Jun. 8, 2005; revision accepted Aug. 11, 2005.

For correspondence or reprints contact: Buck E. Rogers, PhD, Department of Radiation Oncology, Washington University School of Medicine, 4511 Forest Park Blvd., Suite 411, St. Louis, MO 63108.

E-mail: rogers@radonc.wustl.edu

SSTR5) have been cloned, with alternate splicing of SSTR2 to yield SSTR2A and the C-terminally truncated form, SSTR2B (*10*). All of the receptor subtypes have high binding affinity for the natural somatostatin 14 or somatostatin 28 peptides. Somatostatin receptors are members of the G protein–coupled receptor family and have 7 transmembrane-spanning domains consisting of 3 extracellular loops, termed E1, E2, and E3 (*11*). The 5 receptor subtypes are highly homologous between mice and humans and are expressed in the brain, gastrointestinal tract, pancreas, kidneys, and spleen (*12,13*). Human SSTR2A (hereafter referred to as SSTR2) has been used for the imaging of gene transfer by use of γ-camera imaging and SPECT (*14–17*). These previous studies used the radiolabeled somatostatin analogs ^{111}In-diethylenetriaminepentaacetic acid-octreotide (Octreoscan; Mallinckrodt), ^{99m}Tc-P829 (NeoTect; Diatide, Inc.), and ^{99m}Tc-P2045 (Diatide, Inc.) to demonstrate localization in a tumor after intratumoral injection with an adenovirus or intraperitoneal injection with a vaccinia virus carrying the *sstr2* gene.

Because PET is at least 1 order of magnitude more sensitive than SPECT, in part because of the compromise between spatial resolution and sensitivity attributable to the required collimator for SPECT (*18,19*), it would be advantageous to image SSTR2 gene transfer by PET. In recent years, there has been interest in somatostatin analogs radiolabeled with PET radionuclides, such as ^{18}F, ^{86}Y, ^{66,68}Ga, and ^{64}Cu (*20–24*). All of these radionuclides have advantages and disadvantages for use in the labeling of somatostatin analogs. In this study, we used the positron emitter ^{94m}Tc (half-life, 52 min; β^+, 72%; $E_{\beta+max}$, 2.5 MeV) produced with a high specific activity on a biomedical cyclotron (*25*). The somatostatin analog Demotate 1 (Tyr^3-octreotate conjugated to the 1,4,8,11-tetraazaundecane chelator) (Fig. 1) was used for chelation of ^{94m}Tc and targeting to SSTR2. This analog was previously radiolabeled with ^{99m}Tc for γ-camera imaging of SSTR2-positive tumors (*26*). The binding and internalization of ^{94m}Tc-Demotate 1 were evaluated in vitro after infection of cells with an adenovirus (AdHASSTR2) encoding SSTR2 that contains the influenza virus hemagglutinin (HA) sequence at the N terminus of the receptor. The expression of SSTR2 then was evaluated in vivo with tumor-bearing mice in biodistribution and microPET imaging studies. To our knowledge, this is the first study to use PET to evaluate SSTR2 gene transfer.

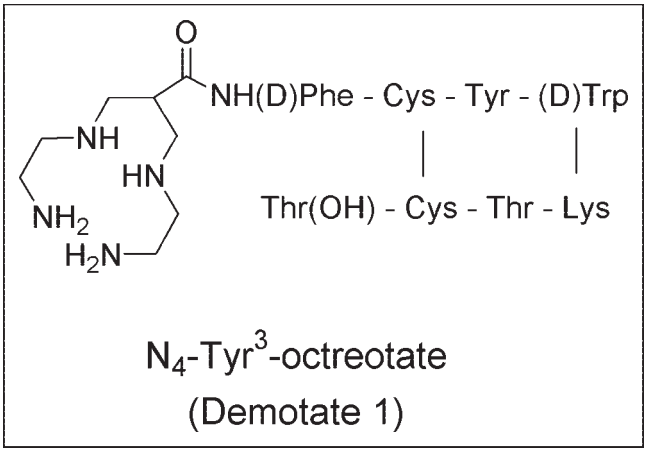

FIGURE 1. Structure of Demotate 1.

MATERIALS AND METHODS

Cell Line and Adenovirus

The A-427 non–small cell lung cancer cell line was purchased from the American Type Culture Collection and maintained in Eagle minimum essential medium supplemented with 1% nonessential amino acids, 1% sodium pyruvate, and 10% heat-inactivated fetal bovine serum. All cell culture reagents were obtained from Invitrogen, except for fetal bovine serum, which was purchased from Sigma Chemical Co. The cells were maintained in a humidified atmosphere with 5% CO_2 at 37°C. AdHASSTR2 was constructed and propagated and virus titers were determined as previously described (*27*), and the virus was stored at −80°C until use in cell culture and animal studies.

Production of ^{94m}Tc

^{94m}Tc was produced by a method similar to that previously described (*25,28,29*). Briefly, MoO_3 (Isoflex USA) (~60 mg), enriched with 91.0% ^{94}Mo, was pressed into a platinum disk and covered with aluminum foil. The disk was irradiated (14.7 MeV, 4 μA, 45 min) on our biomedical cyclotron, and ^{94m}Tc was produced by the ^{94}Mo(p,n)^{94m}Tc nuclear reaction. After irradiation, the ^{94m}Tc was separated by heating of the target in a quartz apparatus at 1,000°C and allowing the ^{94m}Tc to condense in the temperature region of 300°C–400°C. The ^{94m}Tc was removed in NaOH (0.1 mmol/L) and purified over an Alumina N Sep-Pak Light cartridge (Millipore) to yield the desired $^{94m}TcO_4^-$ in saline. The product was >95% $^{94m}TcO_4^-$, as demonstrated by use of instant thin-layer chromatography (ITLC) silica gel plates (Pall Corp.) with acetone as the solvent. The yield of ^{94m}Tc was 1,295 MBq (35 mCi)/μA·h at the end of bombardment (EOB), and isotopic impurities were measured on a multichannel analyzing Ge γ-spectrometer (Canberra). The saline containing $^{94m}TcO_4^-$ was used immediately after isolation for the radiolabeling of Demotate 1.

Synthesis and Radiolabeling of Demotate 1

Demotate 1 was synthesized as previously described (*26*). For radiolabeling, Demotate 1 was dissolved in acetic acid (10 mmol/L) at 2 mg/mL, and 15 μg were added to a vial containing 25 μL of phosphate buffer (0.5 mol/L), 3 μL of trisodium citrate buffer (0.1 mol/L), and 196 MBq (5.3 mCi) of $^{94m}TcO_4^-$ (200 μL). To this solution, 20 μg of $SnCl_2$ (dissolved in ethanol at 5 mg/mL) were added, and the reaction mixture was incubated for 15 min at room temperature. The reaction was stopped by the addition of 4 μL of HCl (1 mol/L) and 25 μL of ethanol. Radiochemical purity was determined by use of ITLC with acetone and 1:1 methanol: ammonium acetate (1 mol/L) as the solvents. The plates were analyzed by use of an imaging scanner (Bioscan), with ^{94m}Tc-Demotate 1 remaining at the origin in the acetone system and moving with the solvent front in the ammonium acetate system.

Saturation Binding Assays

A-427 cells were infected with AdHASSTR2 at 10 plaque-forming units (pfu) per cell and harvested 2 d later to prepare

membrane homogenates as previously described (*30*). Twenty-five micrograms of membrane homogenate were added to each well of a 96-well Multiscreen Durapore filtration plate (Millipore) and rinsed twice with cold buffer [*N*-(2-hydroxyethyl)piperazine-*N*′-(2-ethanesulfonic acid) (HEPES) at 10 mmol/L, $MgCl_2$ at 5 mmol/L, ethylenediaminetetraacetic acid at 1 mmol/L, and 0.1% bovine serum albumin (pH 7.4)]. Various concentrations (0.5−100 nmol/L) of ^{94m}Tc-Demotate 1 were added to the wells in triplicate in the presence or absence of Tyr^1-somatostatin (Sigma Chemical Co.) as an inhibitor such that the final volume in each well was 110 μL. The plate was incubated at room temperature for 30 min with shaking, the wells were rinsed twice with buffer, and the filters were dried and removed. Counts in samples were determined by use of a model 8000 automated well-type γ-counter (Beckman). Data were analyzed by use of the 1-site binding equation in Prism software (GraphPad) to generate equilibrium dissociation constants (K_d) and maximum binding capacities.

Internalization Assays

A-427 cells were infected with AdHASSTR2 at 10 pfu per cell and then used to seed 6-well plates 24 h later. One day after seeding (2 d after adenovirus infection), ^{94m}Tc-Demotate 1 (1 nmol/L) in 1 mL of internalization medium (Dulbecco minimum essential medium, HEPES at 30 mmol/L, L-glutamine at 2 mmol/L, sodium pyruvate at 1 mmol/L, and 1% bovine serum albumin) was added to each well and incubated at 37°C for 5, 15, 30, 60, and 120 min. An excess (>1,000 nmol/L) of Tyr^1-somatostatin was added to half of the wells to demonstrate specific binding and internalization. The cells were rinsed twice with phosphate-buffered saline and then with Hanks balanced salt solution containing sodium acetate at 20 mmol/L (pH 4.0) to remove surface-bound radioactivity. The cells then were harvested with 1 mL of sodium borate (10 mmol/L) containing 10% sodium dodecyl sulfate and counted in the γ-counter along with the acid washes to determine the internalized radioactivity and the cell surface radioactivity. After 24 h, the amount of protein in each well was determined by use of a bicinchoninic acid (BCA) protein assay kit (Pierce). The data are presented as the specific amount of peptide (Tyr^1-somatostatin–blocked wells subtracted from nonblocked wells) bound to the cell surface or internalized, normalized to the amount of protein per well.

Animal Biodistribution Studies

All animal studies were performed in compliance with guidelines for the care and use of research animals established by the Washington University Animal Studies Committee. Homozygous 6- to 8-wk-old female nude (*nu/nu*) mice (Charles River Laboratories, Inc.) were implanted subcutaneously in each rear flank with 10^7 A-427 cells mixed 1:1 with Matrigel (Becton Dickinson) such that each mouse had 2 tumors. Three weeks after tumor cell inoculation, tumors on 1 side of the mice were injected directly with 10^9 pfu (30 μL) of AdHASSTR2, and the other tumors were injected with 10^9 pfu (30 μL) of a control adenovirus (AdGRPR, encoding the gastrin-releasing peptide receptor), as previously described (*31*). Two days after the adenovirus injections, 0.6 MBq (17 μCi; 100 ng) of ^{94m}Tc-Demotate 1 was injected via the tail vein. The mice ($n = 6$) were sacrificed by cervical dislocation 1 and 2 h later. In another experiment, the same procedures were followed, except that 1 group of mice was injected in the tail vein with ^{94m}Tc-Demotate 1 and another group was coinjected with 50 μg of unlabeled Demotate 1 as an inhibitor. Both groups ($n = 5$) were sacrificed 1 h after injection. The blood, lungs, liver, spleen, kidneys, muscle, bone, pancreas, and tumors were harvested, weighed, and counted in the γ-counter. Samples were corrected for radioactive decay to calculate the percentage injected dose per gram (% ID/g) of tissue by comparison with a standard representing the injected dose.

MicroPET Imaging

MicroPET imaging was performed with an R4 microPET scanner (Concorde Microsystems Inc.). The R4 microPET scanner has a field of view of 8 cm axially by 11 cm transaxially and is capable of a spatial resolution of 2.3 mm and an absolute sensitivity of 1,020 counts per second per 0.037 MBq in the middle of the field of view. The same animal model as that described above was used for microPET imaging, except that the tumors were implanted in the axillary thorax. In these studies, the mice ($n = 3$) were injected via the tail vein with 18.5 MBq (500 μCi; 3.4 μg) of ^{94m}Tc-Demotate 1, anesthetized 1 and 2 h later with 1%–2% isoflurane, positioned supine, immobilized, and imaged. The tumor and kidney standard uptake values (SUVs) were generated as previously described (*32*). Briefly, the regions of interest encompassing the entire tumor or tissue on the microPET images were measured to generate the radioactivity concentration, which was decay corrected to the time of injection. This value then was multiplied by the mouse body weight (grams) and divided by the injected dose (Bq) to yield the tissue uptake normalized to injected dose per gram of body weight: (Bq/mL) × (weight [g]/injected dose [Bq]).

Statistical Analysis

All of the data are presented as the mean ± SEM. The Student *t* test (2 tailed) was performed with Prism software to determine statistical significance at the 95% confidence level, with $P < 0.05$ being considered significantly different.

RESULTS

Production of ^{94m}Tc and Radiolabeling of Demotate 1

The major radionuclide impurity of <7% was from ^{94g}Tc (half-life, 293 min; β^+, 10.5%; $E_{\beta+max}$, 811 keV), with all other radionuclide impurities constituting <0.4%. The positron contribution of ^{94g}Tc was not greater than 10% up to 4 h after EOB. The processing time from EOB until $^{94m}TcO_4^-$ was ready for radiolabeling of Demotate 1 was typically 45 min. This process resulted in a recovery of radioactivity that ranged from 81 to 274 MBq (2.2–7.4 mCi) and an effective specific activity for ^{94m}Tc-Demotate 1 of 14,874 ± 4,884 MBq/μmol (402 ± 132 mCi/μmol; $n = 8$). The radiochemical purity of ^{94m}Tc-Demotate 1, as determined with the ITLC system described above, was >95.5%. The total time from EOB until ^{94m}Tc-Demotate 1 was ready for in vitro or in vivo studies was 75 min, and it should be noted that unlabeled Demotate 1 was not separated from ^{94m}Tc-Demotate 1 before use.

Saturation Binding Assays

A representative saturation binding curve and Scatchard transformation are shown in Figures 2A and 2B, respectively. The data show that ^{94m}Tc-Demotate 1 bound to a single class of binding sites with a K_d of 9.6 ± 2.8 nmol/L and a maximum binding capacity of 9,200 ± 2,700 fmol/mg of protein, as determined from 3 independent experiments.

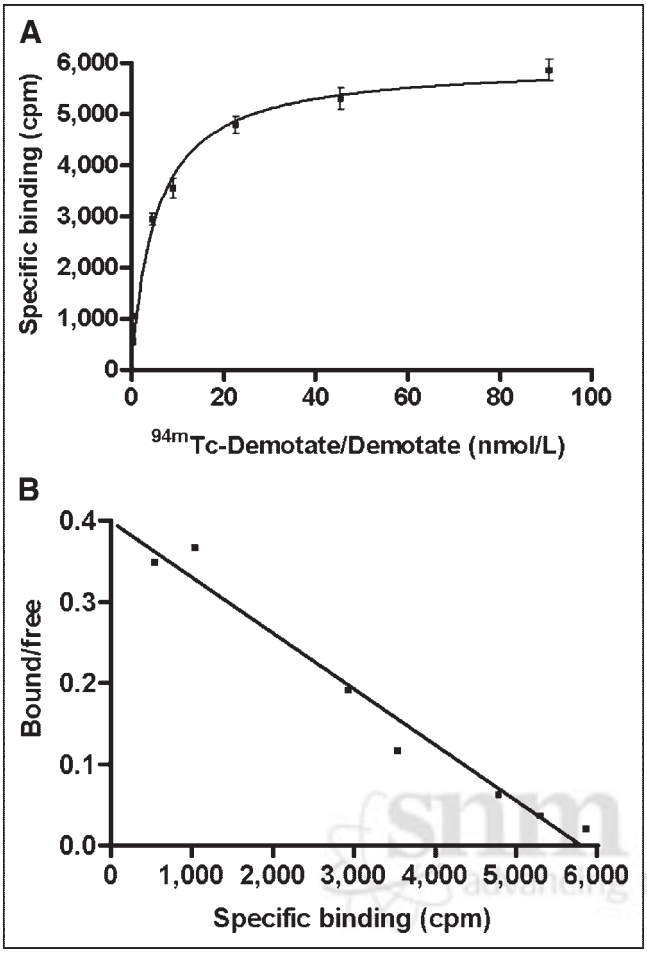

FIGURE 2. Representative plot of ^{94m}Tc-Demotate 1–Demotate 1 saturation binding curve (A) and Scatchard transformation (B) for membrane preparations from A-427 cells infected with AdHASSTR2 at 10 pfu per cell. It should be noted that ^{94m}Tc-Demotate 1 concentrations included unlabeled Demotate 1 and that saturation binding curve represented specific binding (nonspecifically bound subtracted from total bound). Each data point represents mean ± SEM of triplicate measurements.

Because ^{94m}Tc-Demotate 1 consists of a mixture of radiolabeled Demotate 1 and unlabeled Demotate 1, the K_d represents a composite of these 2 species.

Internalization Assays

A-427 cells infected with AdHASSTR2 at 10 pfu per cell demonstrated time-dependent internalization of ^{94m}Tc-Demotate 1 (Fig. 3). The amount of specifically internalized ^{94m}Tc-Demotate 1 was 285 fmol/mg of protein at 5 min and increased to 1,022, 1,558, 1,842, and 2,407 fmol/mg at 15, 30, 60, and 120 min, respectively. The amount of internalized ^{94m}Tc-Demotate 1 was significantly greater ($P < 0.0001$) at all time points than the amount of surface-bound ^{94m}Tc-Demotate 1 (<182 fmol/mg at all time points), except for the 5-min time point.

Animal Biodistribution Studies

The tissue uptake of ^{94m}Tc-Demotate 1 in tumor-bearing mice receiving intratumoral injections of AdHASSTR2 is shown in Figure 4A. The uptake of ^{94m}Tc-Demotate 1 in tumors injected with AdHASSTR2 was 3.5 ± 0.8 %ID/g and 4.0 ± 0.6 %ID/g at 1 and 2 h after the administration of ^{94m}Tc-Demotate 1, respectively. This uptake was significantly higher ($P < 0.03$) than the uptake at both time points in all other tissues, except for the kidneys, the SSTR2-positive pancreas, and the liver at 1 h. There was rapid blood clearance of ^{94m}Tc-Demotate 1, with 1.2 ± 0.1 %ID/g remaining at 1 h and 0.8 ± 0.1 %ID/g remaining at 2 h. The uptake of ^{94m}Tc-Demotate 1 was <1.8 %ID/g in all other tissues, except for the pancreas, kidneys, and SSTR2-positive tumors at both time points. The ratios for the AdHASSTR2-injected tumors and other tissues at 1 and 2 h are shown in Figure 4B. The data show that all of the ratios were >2 at both time points, except for the kidney and pancreas ratios, which were both <1. The ratios also all increased from 1 h to 2 h in all tissues.

SSTR2-mediated uptake of ^{94m}Tc-Demotate 1 in tumors injected with AdHASSTR2 was demonstrated by coinjection of an excess of unlabeled Demotate 1 and by comparison with a tumor injected with AdGRPR as a control adenovirus (Table 1). The blocking study showed a significant decrease ($P < 0.003$) in the SSTR2-positive tumor uptake of ^{94m}Tc-Demotate 1 at 1 h (5.4 ± 0.8 %ID/g) with coinjection of the blocking agent (1.6 ± 0.3 %ID/g). The tumor injected with AdGRPR showed ^{94m}Tc-Demotate 1 uptake that ranged from 0.8 ± 0.1 %ID/g (Table 1) to 1.5 ± 0.3 %ID/g (Fig. 4A) at 1 h and was 0.8 ± 0.1 %ID/g at 2 h; these uptake values were significantly lower ($P < 0.03$) than the uptake values at those time points for the AdHASSTR2-

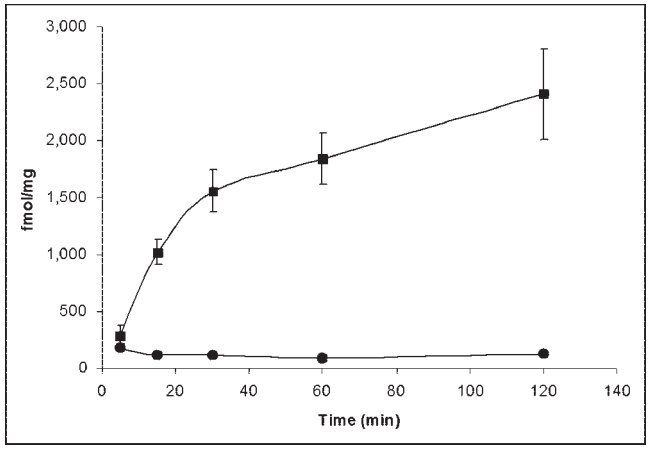

FIGURE 3. Specific internalization at 37°C of ^{94m}Tc-Demotate 1 into A-427 cells infected with AdHASSTR2 at 10 pfu per cell. ^{94m}Tc-Demotate 1 (1 nmol/L) was incubated with cells for various times in presence or absence of inhibitor. Cells were acid washed to remove surface-bound radioactivity and then were harvested to determine internalized radioactivity. Specific internalized radioactivity (internalized with inhibitor subtracted from internalized without inhibitor) (■) and specific surface-bound radioactivity (surface bound with inhibitor subtracted from surface bound without inhibitor) (●) are shown. Data for each time point are presented as mean ± SEM of 2–5 experiments each performed in triplicate.

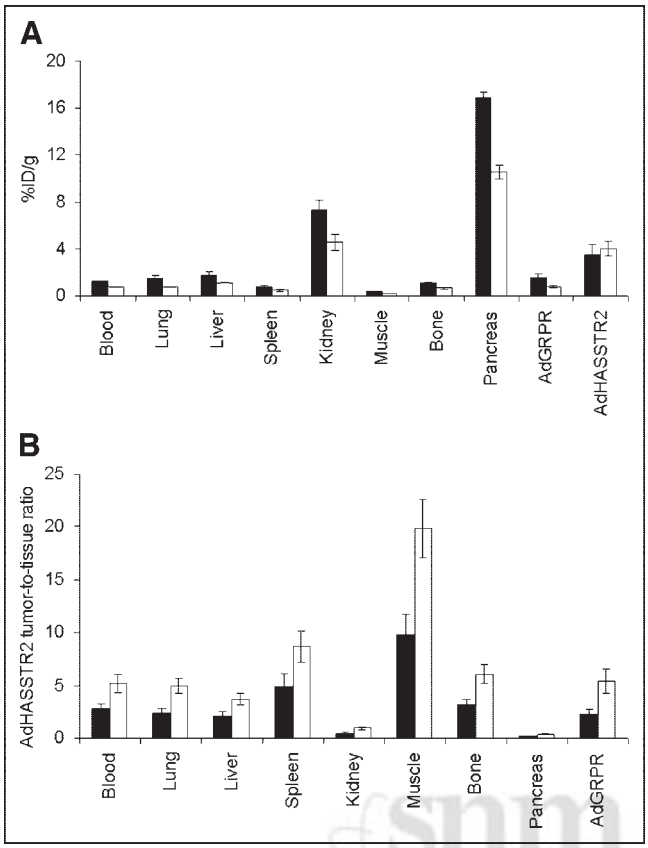

FIGURE 4. Biodistribution of ^{94m}Tc-Demotate 1 in mice bearing A-427 tumor xenografts. Tumors were injected directly with either AdHASSTR2 or AdGRPR as control, and ^{94m}Tc-Demotate 1 was injected via tail vein 2 d later. Mice were sacrificed 1 h (■) and 2 h (□) later ($n = 6$ for each group). Data are presented as mean ± SEM %ID/g for each type of tissue (A) and as ratio of AdHASSTR2-injected tumor uptake to tissue uptake at both time points (B).

injected tumors. The uptake of ^{94m}Tc-Demotate 1 also significantly decreased ($P < 0.0001$) from 21.3 ± 1.5 %ID/g without the blocking agent to 0.2 ± 0.03 %ID/g with the blocking agent in the pancreas. The only other tissues to show a significant decrease after administration of the blocking agent were the liver ($P < 0.02$) and the kidneys ($P = 0.045$). In addition, the radioactivity in the pancreas decreased 37% from 1 h to 2 h compared with no decrease in SSTR2-positive tumors. This finding likely was attributable to the high enzymatic activity in the pancreas, which led to higher tumor-to-pancreas uptake ratios at later time points. The only significant differences in the uptake of ^{94m}Tc-Demotate 1 between the 2 experiments conducted at 1 h (Fig. 4A; Table 1) were found in the blood, pancreas, and AdGRPR-injected tumor.

MicroPET Imaging

Tumor-bearing mice were imaged 1 and 2 h after the injection of ^{94m}Tc-Demotate 1, and 1-h coronal and transaxial microPET images are shown in Figures 5A and 5B, respectively. The data show clear uptake of ^{94m}Tc-Demotate 1 in the axillary tumor injected with AdHASSTR2 and background uptake in the tumor injected with AdGRPR. Also, as in the biodistribution studies, the clearance of radioactivity through the kidneys and excretion through the bladder were clearly visualized. The pancreas was not observed in Figure 5 because of the slice of the microPET image shown. SUVs also were determined for both tumors and the kidneys (Fig. 5C). The data show that there was significantly greater ($P < 0.007$) uptake of ^{94m}Tc-Demotate 1 in the AdHASSTR2-injected tumor than in the AdGRPR-injected tumor at both time points and that the uptake in the kidneys was significantly greater ($P < 0.02$) than the uptake in the AdHASSTR2-injected tumor at both time points. Comparison of the uptake in the AdHASSTR2-injected tumor with that in the AdGRPR-injected tumor and with that in the kidneys (by SUV and biodistribution analyses) is shown in Figure 5D. There was good agreement between the SUV analysis and the biodistribution analysis at 1 and 2 h for the ratio of the AdHASSTR2-injected tumor uptake to the AdGRPR-injected tumor uptake. These values differed by <12% at each time point. The differences between the SUV and biodistribution analyses were greater when the AdHASSTR2-injected tumor uptake was compared with the kidney uptake. A 35% difference between the values was observed at 1 h, whereas a 65% difference was observed at 2 h.

DISCUSSION

Initial studies of imaging of gene transfer with the SSTR2 gene as a reporter gene were carried out with probes radiolabeled with γ-emitters for γ-camera or SPECT analysis (*14–17*). These studies were carried out with ^{99m}Tc- or ^{111}In-labeled probes for evaluating the tumor expression of SSTR2 after animals were administered a gene therapy vector carrying the *sstr2* gene. SSTR2-specific uptake of these probes was observed in the tumors after direct injection of adenovirus vectors into the tumors or intraperitoneal injection of a vaccinia virus. In addition, Rogers et al. evaluated an adenovirus that contains SSTR2 with the 9-amino-acid HA sequence inserted in the N terminus of the receptor (*27*). That study demonstrated that insertion of the HA sequence into the N terminus of SSTR2 did not have an adverse effect on ligand binding to SSTR2 and that the HA sequence could serve as an alternative epitope for the binding of anti-HA antibodies. However, because PET has better sensitivity than SPECT at a given resolution, this system could be improved through the use of probes radiolabeled with positron emitters.

^{94m}Tc has the same chemistry as the γ-emitter ^{99m}Tc (the most important γ-emitting radionuclide) but is a positron emitter that can be used for PET studies. It is readily produced on a biomedical cyclotron at high specific activities for the radiolabeling of various biomolecules. Nickles et al. showed that ^{94m}Tc could be used in myocardial perfusion studies to obtain results that correlated well with those of standard PET perfusion studies (*33*). Griffiths et al.

TABLE 1
Biodistribution ($n = 5$) of ^{94m}Tc-Demotate 1 in Mice Bearing A-427 Tumor Xenografts Directly Injected with AdHASSTR2 or AdGRPR*

Tissue	Mean ± SEM %ID/g for: Unblocked samples	Blocked samples
Blood	0.37 ± 0.05	0.41 ± 0.09
Lungs	1.16 ± 0.27	0.59 ± 0.08
Liver	1.37 ± 0.23	0.64 ± 0.06†
Spleen	0.56 ± 0.16	0.24 ± 0.02
Kidneys	9.43 ± 1.13	5.90 ± 0.97†
Muscle	0.27 ± 0.08	0.33 ± 0.09
Bone	1.09 ± 0.34	0.30 ± 0.04
Pancreas	21.31 ± 1.53	0.22 ± 0.03†
AdGRPR-injected tumors	0.82 ± 0.06	1.33 ± 0.18
AdHASSTR2-injected tumors	5.39 ± 0.84	1.56 ± 0.26†

*Mice were sacrificed 1 h after intravenous injection of ^{94m}Tc-Demotate 1 with or without coinjection of 50 μg of unlabeled Demotate 1 as blocking agent.

†Value for blocked sample was significantly lower ($P < 0.05$) than value for unblocked sample.

showed that an Fab′ fragment of an anti–carcinoembryonic antigen monoclonal antibody could be readily radiolabeled with ^{94m}Tc for potential PET of carcinoembryonic antigen–positive tumors (*34*). Luyt et al. used ^{94m}Tc to radiolabel an estrogen derivative to evaluate estrogen receptor expression in rats by microPET imaging (*25*). The advantages of using ^{94m}Tc over other positron emitters are that it has a relatively simple chemistry for the labeling of peptides and antibodies (compared with ^{18}F, ^{76}Br, or ^{124}I), imaging studies must be conducted on the same day as radiopharmaceutical administration because of the short half-life (this is not necessarily true for longer-lived isotopes), and the short half-life should lead to radiation doses lower than those observed with longer-lived isotopes. However, ^{94m}Tc requires a biomedical cyclotron for production and has less-than-ideal physical properties for PET because of the high positron energy. This high positron energy leads to an intrinsic spatial resolution loss of 3.3 mm (*35*) but is still expected to provide resolution superior to that of corresponding studies with ^{99m}Tc and SPECT (*34*). Thus, ^{94m}Tc-labeled biomolecules can be used to model tracer kinetics, measure dosimetry, and determine structure–activity relationships by PET before their wider application with ^{99m}Tc and SPECT.

In this study, ^{94m}Tc was used to radiolabel the somatostatin analog Demotate 1. Demotate 1 was previously radiolabeled with ^{99m}Tc and has demonstrated good SSTR2-mediated tumor uptake in preclinical and clinical studies (*26,36*). These studies showed that tumor uptake could be observed within 15 min of ^{99m}Tc-Demotate 1 injection and that maximum tumor uptake and tumor/organ uptake ratios could be observed by 1 h after injection. These data are important for the radiolabeling of Demotate 1 with ^{94m}Tc because its 52-min half-life requires rapid target tissue uptake and

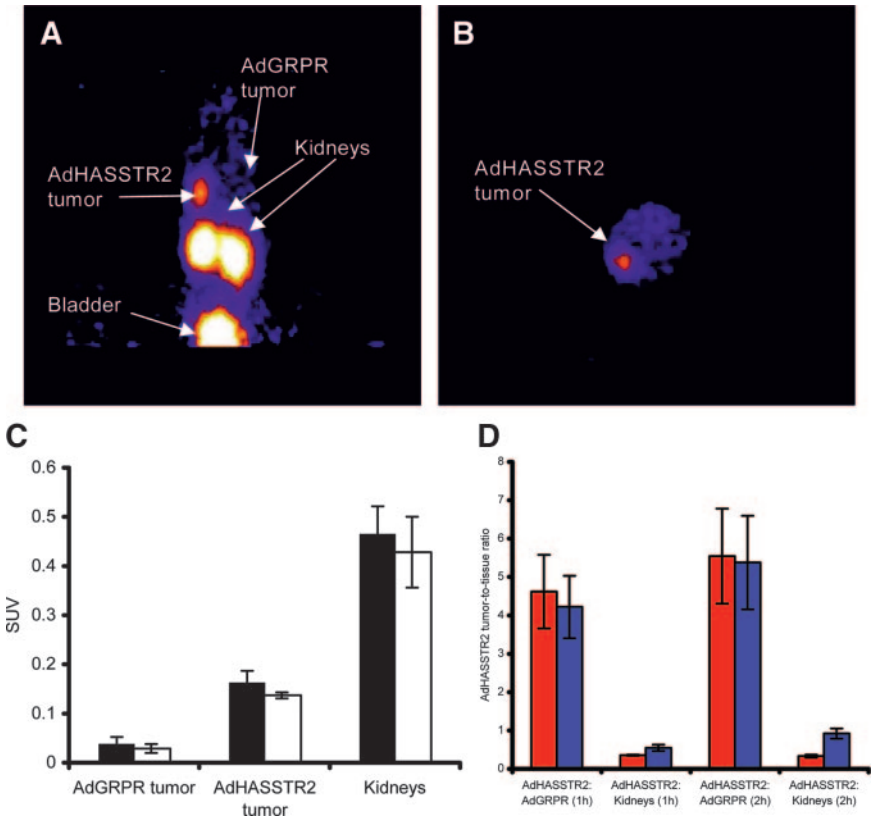

FIGURE 5. (A and B) Coronal (A) and transaxial (B) microPET projection images of A-427 tumor–bearing mice at 1 h after injection of ^{94m}Tc-Demotate 1. Mice carried axillary tumors in which left tumor was injected directly with AdHASSTR2 and right tumor was injected with AdGRPR. Coronal image shows uptake of ^{94m}Tc-Demotate 1 in AdHASSTR2-injected tumor and clearance through kidneys and bladder but background uptake in AdGRPR-injected tumor. (C) SUVs obtained from microPET images for AdGRPR-injected tumors, AdHASSTR2-injected tumors, and kidneys in 3 mice at 1 h (■) and 2 h (□). (D) Ratios of uptake in AdHASSTR2-injected tumors to that in AdGRPR-injected tumors and of uptake in AdHASSTR2-injected tumors to that in kidneys, as determined by SUV analysis (red bars; $n = 3$) and biodistribution analysis (blue bars; $n = 11$ for 1 h and $n = 6$ for 2 h). Data in C and D are presented as mean ± SEM.

clearance from nontarget organs. Radiolabeling of Demotate 1 with ^{94m}Tc was accomplished with high radiochemical purity in 15 min with an effective specific activity of 14,800 MBq/μmol (400 mCi/μmol). The effective specific activity was not optimized in our studies because we used 15 μg of Demotate 1 for all of the radiolabelings and never more than 273.8 MBq (7.4 mCi) of ^{94m}Tc. Therefore, it is expected that higher effective specific activities can be achieved by optimizing these parameters.

The saturation studies (Fig. 2) showed that ^{94m}Tc-Demotate 1 binds with a high affinity (9.6 nmol/L) to A-427 cells infected with AdHASSTR2 at 10 pfu per cell. Maina et al. showed that ^{99m}Tc-Demotate bound to SSTR2-expressing AR42J rat pancreatic carcinoma cells with a K_d that was approximately 100 times higher (70 pmol/L) (*26*). This result likely was attributable to ^{99m}Tc-Demotate having a higher affinity for SSTR2 than unlabeled Demotate. This finding is similar to the findings of studies showing that somatostatin analogs complexed with Tc/Re have a 20- to 30-fold higher affinity than noncomplexed analogs (*37*). In these saturation studies, Maina et al. ensured that all of the Demotate contained a Tc atom by using ^{99g}Tc as a carrier so that the final product was $^{99m/99g}$Tc-Demotate. Because of the short half-life of ^{94m}Tc, we chose not to add ^{99g}Tc as a carrier and performed the studies with a mixture of ^{94m}Tc-Demotate 1 and unlabeled Demotate 1. This mixture is similar to many ^{99m}Tc "kit" formulations of radiopharmaceutical agents that contain an excess of the biomolecule. The expression of SSTR2 in A-427 cells infected with AdHASSTR2 at 10 pfu per cell in this study (~9,200 fmol/mg) was similar to that previously described (~33,000 fmol/mg) (*27*). These values for SSTR2 expression are 50–100 times higher than those reported with the commonly used AR42J cell line.

Rapid internalization of ^{94m}Tc-Demotate 1 was observed (Fig. 3), with 285 fmol/mg being internalized by 5 min. This internalization increased over the time course of the experiment, with 2,407 fmol/mg being internalized by 2 h. Nonlinear curve fitting showed that the curve reached a maximum at ~3,300 fmol/mg. The initial velocity of internalization at this concentration of ^{94m}Tc-Demotate 1 was ~49.7 fmol/mg/min, as determined by linear regression ($r^2 = 0.96$) over the first 30 min. The amount internalized was greater than the amount surface bound, which remained constant over the course of the experiment. These results are similar to those reported previously for the internalization of ^{99m}Tc-Demotate 1 into AR42J cells, which showed rapid internalization that started to plateau by 15 min and reached its maximum by 30 min. Rapid internalization of radiolabeled peptides has been shown to be important for them to be used as diagnostic or therapeutic agents.

Biodistribution studies showed that there was good uptake of ^{94m}Tc-Demotate 1 in tumors injected with AdHASSTR2, with values of 3.5–5.4 %ID/g at 1 h after injection and 4.0 %ID/g at 2 h. This tumor uptake was comparable to that in other studies with the same A-427 tumor model and an intratumoral injection of adenovirus. Zinn et al. showed that at 48 h after the intratumoral injection of an adenovirus expressing SSTR2, tumor uptake at 3 h after the injection of ^{99m}Tc-P829 was 2.5 %ID/g (*14*). In another study by Zinn et al., 10.2 %ID/g was observed in tumors at 26 h after the injection of ^{99m}Tc-P2045 (*15*). Maina et al. (*26*) showed greater uptake of ^{99m}Tc-Demotate in AR42J cells at 1 h after injection (~25 %ID/g) than was found in AdHASSTR2-infected A-427 cells in this study. This difference in uptake may be explained by the fact that only ~10% of A-427 cells express SSTR2 after adenovirus infection compared with all natively expressing AR42J cells (*14*). Also, as discussed earlier, the specific activity of ^{94m}Tc-Demotate 1 was not optimized in our studies, a factor that may have led to lower tumor uptake, and was ~2.5-fold lower than the specific activity described for ^{99m}Tc-Demotate 1. It is also clear from these studies that tumor uptake was SSTR2 mediated. The reduction in the liver and kidneys after coinjection of the blocking agent may have been attributable to low levels of expression of SSTR2 in these tissues. SSTR2 messenger RNA has been detected in mouse kidneys and liver, with SSTR2 protein being detected in the glomeruli of the kidneys (*38,39*).

As discussed above, several somatostatin analogs have been evaluated for γ-imaging of SSTR2-mediated gene transfer. This is the first study to use a somatostatin analog radiolabeled with a positron emitter to monitor SSTR2-mediated gene transfer by PET. Figures 5A and 5B clearly show the accumulation of ^{94m}Tc-Demotate 1 in tumors infected with AdHASSTR2 and background radioactivity in tumors infected with the control, AdGRPR. As in the biodistribution studies, the kidneys also were observed, with subsequent clearance through the bladder. The pancreas was not observed in these particular slices of the microPET images, but a strong pancreatic signal was observed in others (data not shown), a finding also consistent with the findings of the biodistribution studies. Analysis of the microPET images showed that there was good agreement between the SUVs obtained from microPET studies and the % ID/g values obtained from biodistribution studies. The SUV relationship between AdHASSTR2-injected tumor and the kidney is not as consistent with the biodistribution as the relationship with the control tumor, possibly because of the high levels of radioactivity in the kidneys and the high positron energy of ^{94m}Tc making the SUV measurements in the kidneys less accurate.

It is anticipated that these studies will be expanded to use somatostatin analogs radiolabeled with other positron emitters. Because ^{94m}Tc has a short half-life and is not commonly produced on most cyclotrons, other positron emitters will have more widespread applicability. The ^{18}F-labeled somatostatin analogs could be used at most institutions with cyclotrons but still suffer from a relatively complex synthesis strategy (*23,40*). Somatostatin analogs radiolabeled with ^{86}Y or ^{64}Cu have the advantage of the long half-life of these isotopes for regional shipping and imaging at later time points, whereas ^{68}Ga has the advantage of being generator

produced for use at many institutions. Nevertheless, these studies demonstrate that ^{94m}Tc-Demotate 1 can be used for PET of SSTR2-mediated gene transfer and that ^{94m}Tc-Demotate 1 could be used to model gene transfer characteristics with PET before radiolabeling with ^{99m}Tc for additional SPECT studies.

CONCLUSION

This study shows that SSTR2-mediated gene transfer can be monitored by PET. Specific tumor localization of ^{94m}Tc-Demotate 1 in mice was visualized by microPET imaging after intratumoral injection of AdHASSTR2 but not after intratumoral injection of a control adenovirus. This investigation represents a first step in demonstrating that SSTR2 can serve as a reporter probe for PET gene transfer. The use of somatostatin analogs radiolabeled with other positron emitters and the development of better ligands that target the HA epitope may improve this system further.

ACKNOWLEDGMENTS

This work was supported by Department of Energy grant DE-FG02-02ER63476 and the Department of Radiation Oncology, Washington University School of Medicine. The production of ^{94m}Tc at Washington University School of Medicine was supported by NCI grant R24 CA86307. Small-animal imaging at Washington University School of Medicine was supported by NIH grant 5 R24 CA83060. The authors gratefully acknowledge Dr. Petros Sotiriou for his contribution to the synthesis of Demotate 1, Deborah Sultan for the production of ^{94m}Tc, Nicole Fettig for the biodistribution studies, Ron Chen for tumor cell implantation, and Jerrel Rutlin and Lori Strong for the microPET imaging and data analysis. Heather Bigott is also thanked for helpful discussions on the production of ^{94m}Tc, and Carolyn Anderson is thanked for critical reading of the manuscript.

REFERENCES

1. McCormick F. Cancer gene therapy: fringe or cutting edge? *Nat Rev Cancer*. 2001;1:130–141.
2. Sangro B, Qian C, Ruiz J, Prieto J. Tracing transgene expression in cancer gene therapy: a requirement for rational progress in the field. *Mol Imaging Biol*. 2002;4:27–33.
3. Blasberg R. PET imaging of gene expression. *Eur J Cancer*. 2002;38:2137–2146.
4. Tjuvajev JG, Avril N, Oku T, et al. Imaging herpes virus thymidine kinase gene transfer and expression by positron emission tomography. *Cancer Res*. 1998;58:4333–4341.
5. Gambhir SS, Herschman HR, Cherry SR, et al. Imaging transgene expression with radionuclide imaging technologies. *Neoplasia*. 2000;2:118–138.
6. Liang Q, Satyamurthy N, Barrio JR, et al. Noninvasive, quantitative imaging in living animals of a mutant dopamine D2 receptor reporter gene in which ligand binding is uncoupled from signal transduction. *Gene Ther*. 2001;8:1490–1498.
7. Auricchio A, Acton PD, Hildinger M, et al. In vivo quantitative noninvasive imaging of gene transfer by single-photon emission computerized tomography. *Hum Gene Ther*. 2003;10:255–261.
8. Dingli D, Russell SJ, Morris JC, III. In vivo imaging and tumor therapy with the sodium iodide symporter. *J Cell Biochem*. 2003;90:1079–1086.
9. Shen DH, Marsee DK, Schaap J, et al. Effects of dose, intervention time, and radionuclide on sodium iodide symporter (NIS)-targeted radionuclide therapy. *Gene Ther*. 2004;11:161–169.
10. Bell G, Reisine T. Molecular biology of somatostatin receptors. *Trends Neurosci*. 1993;16:34–38.
11. Zinn KR, Chaudhuri TR. The type 2 human somatostatin receptor as a platform for reporter gene imaging. *Eur J Nucl Med*. 2002;29:388–399.
12. Yamada Y, Post SR, Wang K, Tager HS, Bell GI, Seino S. Cloning and functional characterization of a family of human and mouse somatostatin receptors expressed in brain, gastrointestinal tract, and kidney. *Proc Natl Acad Sci USA*. 1992;89:251–255.
13. Feuerbach D, Fehlmann D, Nunn C, et al. Cloning, expression and pharmacological characterisation of the mouse somatostatin sst(5) receptor. *Neuropharmacology*. 2000;39:1451–1462.
14. Zinn KR, Buchsbaum DJ, Chaudhuri T, Mountz JM, Kirkman RL, Rogers BE. Noninvasive monitoring of gene transfer using a reporter receptor imaged with a high-affinity peptide radiolabeled with ^{99m}Tc or ^{188}Re. *J Nucl Med*. 2000;41:887–895.
15. Zinn KR, Chaudhuri TR, Krasnykh VN, et al. Gamma camera dual imaging with a somatostatin receptor and thymidine kinase after gene transfer with a bicistronic adenovirus in mice. *Radiology*. 2002;223:417–425.
16. Buchsbaum DJ, Chaudhuri TR, Yamamoto M, Zinn KR. Gene expression imaging with radiolabeled peptides. *Ann Nucl Med*. 2004;18:275–283.
17. McCart JA, Mehta N, Scollard D, et al. Oncolytic vaccinia virus expressing the human somatostatin receptor SSTR2: molecular imaging after systemic delivery using ^{111}In-pentetreotide. *Mol Ther*. 2004;10:553–561.
18. Budinger T. Single photon emission computed tomography. In: Sandler M, ed. *Diagnostic Nuclear Medicine*. Baltimore, MD: Williams & Wilkins; 1996:121–138.
19. Massoud TF, Gambhir SS. Molecular imaging in living subjects: seeing fundamental biological processes in a new light. *Genes Dev*. 2003;17:545–580.
20. Li WP, Lewis JS, Kim J, et al. DOTA-D-Tyr(1)-octreotate: a somatostatin analogue for labeling with metal and halogen radionuclides for cancer imaging and therapy. *Bioconjug Chem*. 2002;13:721–728.
21. Kowalski J, Henze M, Schuhmacher J, Macke HR, Hofmann M, Haberkorn U. Evaluation of positron emission tomography imaging using [^{68}Ga]-DOTA-D Phe^1-Tyr^3-octreotide in comparison to [^{111}In]-DTPAOC SPECT: first results in patients with neuroendocrine tumors. *Mol Imaging Biol*. 2003;5:42–48.
22. Jamar F, Barone R, Mathieu I, et al. ^{86}Y-DOTA^0-D-Phe^1-Tyr^3-octreotide (SMT487): a phase 1 clinical study—pharmacokinetics, biodistribution and renal protective effect of different regimens of amino acid co-infusion. *Eur J Nucl Med Mol Imaging*. 2003;30:510–518.
23. Wester HJ, Schottelius M, Scheidhauer K, et al. PET imaging of somatostatin receptors: design, synthesis and preclinical evaluation of a novel ^{18}F-labelled, carbohydrated analogue of octreotide. *Eur J Nucl Med Mol Imaging*. 2003;30:117–122.
24. Uger O, Kothari PJ, Finn RD, et al. Ga-66 labeled somatostatin analogue DOTA-DPhe^1-Tyr^3-octreotide as a potential agent for positron emission tomography imaging and receptor mediated internal radiotherapy of somatostatin receptor positive tumors. *Nucl Med Biol*. 2002;29:147–157.
25. Luyt LG, Bigott HM, Welch MJ, Katzenellenbogen JA. 7α- and 17α-Substituted estrogens containing tridentate tricarbonyl rhenium/technetium complexes: synthesis of estrogen receptor imaging agents and evaluation using microPET with technetium-94m. *Bioorg Med Chem*. 2003;11:4977–4989.
26. Maina T, Nock B, Nikolopoulou A, et al. [^{99m}Tc]Demotate, a new ^{99m}Tc-based [Tyr^3]octreotate analogue for the detection of somatostatin receptor-positive tumours: synthesis and preclinical results. *Eur J Nucl Med Mol Imaging*. 2002;29:742–753.
27. Rogers BE, Chaudhuri TR, Reynolds PN, Della Manna D, Zinn KR. Noninvasive gamma camera imaging of gene transfer using an adenoviral vector encoding an epitope tagged receptor as a reporter. *Gene Ther*. 2003;10:105–114.
28. Rosch F, Novgorodov AF, Qaim SM. Thermochromatographic separation of ^{94m}Tc from enriched molybdenum targets and its large scale production for nuclear medical applications. *Radiochim Acta*. 1994;64:113–120.
29. Qaim SM. Production of high purity ^{94m}Tc for positron emission tomography studies. *Nucl Med Biol*. 2000;27:323–328.
30. Rogers BE, McLean SF, Kirkman RL, et al. *In vivo* localization of [^{111}In]-DTPA-D-Phe^1-octreotide to human ovarian tumor xenografts induced to express the somatostatin receptor subtype 2 using an adenoviral vector. *Clin Cancer Res*. 1999;5:383–393.
31. Rogers BE, Rosenfeld ME, Khazaeli MB, et al. Localization of iodine-125-mIP-Des-Met^{14}-bombesin (7–13)NH_2 in ovarian carcinoma induced to express the gastrin releasing peptide receptor by adenoviral vector–mediated gene transfer. *J Nucl Med*. 1997;38:1221–1229.
32. McQuade P, Knight LC, Welch MJ. Evaluation of ^{64}Cu- and ^{125}I-radiolabeled bitistatin as potential agents for targeting αv β3 integrins in tumor angiogenesis. *Bioconjug Chem*. 2004;15:988–996.

33. Nickles RJ, Nunn AD, Stone CK, Christian BT. Technetium-94m-teboroxime: synthesis, dosimetry and initial PET imaging studies. *J Nucl Med.* 1993;34:1058–1066.
34. Griffiths GL, Goldenberg DM, Roesch F, Hansen HJ. Radiolabeling of an anticarcinoembryonic antigen antibody Fab′ fragment (CEA-Scan) with the positron-emitting radionuclide Tc-94m. *Clin Cancer Res*. 1999;5(suppl):3001s–3003s.
35. Pagani M, Stone-Elander S, Larsson SA. Alternative positron emission tomography with non-conventional positron emitters: effects of their physical properties on image quality and potential clinical applications. *Eur J Nucl Med*. 1997;24:1301–1327.
36. Decristoforo C, Maina T, Nock B, Gabriel M, Cordopatis P, Moncayo R. ^{99m}Tc-Demotate 1: first data in tumour patients—results of a pilot/phase I study. *Eur J Nucl Med Mol Imaging*. 2003;30:1211–1219.
37. Vallabhajosula S, Moyer BR, Lister-James J, et al. Preclinical evaluation of technetium-99m-labeled somatostatin receptor–binding peptides. *J Nucl Med*. 1996;37:1016–1022.
38. Bates CM, Kegg H, Grady S. Expression of somatostatin receptors 1 and 2 in the adult mouse kidney. *Regul Pept.* 2004;119:11–20.
39. Hofland LJ, Lamberts SW, van Hagen PM, et al. Crucial role for somatostatin receptor subtype 2 in determining the uptake of [^{111}In-DTPA-D-Phe^{1}]octreotide in somatostatin receptor–positive organs. *J Nucl Med*. 2003;44:1315–1321.
40. Schottelius M, Poethko T, Herz M, et al. First (18)F-labeled tracer suitable for routine clinical imaging of sst receptor-expressing tumors using positron emission tomography. *Clin Cancer Res*. 2004;10:3593–3606.